THE JOURNAL OF PHYSICAL CHEMISTRY LETTERS
A JOURNAL OF THE AMERICAN CHEMICAL SOCIETY

pubs.acs.org/JPCL

Letter

Induced Migration of CO_2 from Hydrate Cages to Amorphous Solid Water under Ultrahigh Vacuum and Cryogenic Conditions

Gaurav Vishwakarma, Bijesh K. Malla, K. S. S. V. Prasad Reddy, Jyotirmoy Ghosh, Soham Chowdhury, Sharma S. R. K. C. Yamijala, Sandeep K. Reddy,* Rajnish Kumar,* and Thalappil Pradeep*

Cite This: *J. Phys. Chem. Lett.* 2023, 14, 2823−2829

Read Online

ACCESS | Metrics & More | Article Recommendations | Supporting Information

ABSTRACT: Restricted migration of reactive species limits chemical transformations within interstellar and cometary ices. We report the migration of CO_2 from clathrate hydrate (CH) cages to amorphous solid water (ASW) in the presence of tetrahydrofuran (THF) under ultrahigh vacuum (UHV) and cryogenic conditions. Thermal annealing of sequentially deposited CO_2 and H_2O ice, CO_2@H_2O, to 90 K resulted in the partitioning of CO_2 in 5^{12} and $5^{12}6^2$ CH cages (CO_2@5^{12}, CO_2@$5^{12}6^2$). However, upon preparing a composite ice film composed of CO_2@5^{12}, CO_2@$5^{12}6^2$ and THF distributed in the water matrix at 90 K, and annealing the mixture for 6 h at 130 K produced mixed CO_2−THF CH, where THF occupied the $5^{12}6^4$ cages (THF@$5^{12}6^4$) exclusively while CO_2 in $5^{12}6^2$ cages (CO_2@$5^{12}6^2$) got transferred to the ASW matrix and CO_2 in the 5^{12} cages (CO_2@5^{12}) remained as is. This cage−matrix exchange may create a more conducive environment for chemical transformations in interstellar environments.

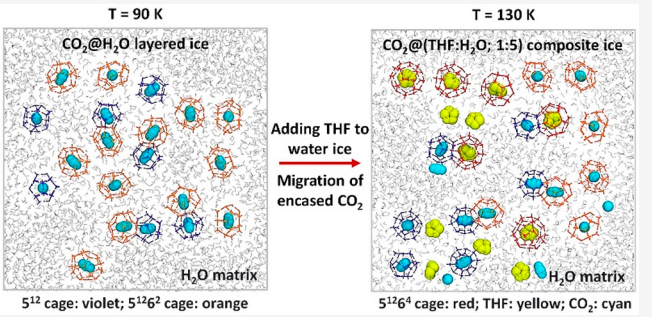

The existence of clathrate hydrates (CHs) under high and ultrahigh vacuum (UHV) and cryogenic conditions is now well established.[1−17] While CH of CO_2 at 120 K in a vacuum of 10^{-6} to 10^{-7} Torr has been known since 1991,[12] the formation of CHs of CH_4,[6,18] C_2H_6,[14] CO_2,[6,18] acetone,[15] formaldehyde,[16] and tetrahydrofuran (THF)[13] in UHV has been observed in the past few years in the range of 10−130 K. CHs are crystalline host−guest inclusion compounds and have drawn wide interest due to their scientific and technological implications.[19−21] CHs often coexist along with water ice and are mainly classified into structures I (sI, consisting of two small 5^{12} and six large $5^{12}6^2$ cages per unit cell) and II (sII, consisting of 16 small 5^{12} and eight large $5^{12}6^4$ cages per unit cell). While CO_2 is known to be encased in small 5^{12} and large $5^{12}6^2$ cages, THF due to its larger van der Waals radius occupies the large $5^{12}6^4$ cage exclusively.[2,9,13,22] In UHV, spectroscopic signatures of molecules in different hydrate cages (5^{12}, $5^{12}6^2$, and $5^{12}6^4$) were reported,[6,13−16] although these structures have not been confirmed by X-ray diffraction experiments. However, in a high vacuum, in situ synchrotron X-ray diffraction experiments have been used to establish the existence of CHs of CH_4 and CO_2.[8] Various CHs could exist along with the water matrix, although their extended crystalline phase has not been observed, in UHV. The presence of CH nuclei in the nanometric domain suggests the coexistence of various phases such as CH, amorphous ice, and dilute solutions of molecules under UHV and cryogenic conditions.[14]

The dynamics of host and guest molecules in CHs have been studied, revealing the reorientation of water and diffusion of guest molecules.[23−29] Moudrakovski et al.,[27] by choosing two sets of guest pairs, THF−CO_2 and isobutane−CO_2, have shown that the coupled motions of water and CO_2 are faster in the former case when THF and CO_2 occupy the large ($5^{12}6^4$) and small (5^{12}) cages of sII hydrate, respectively. They have also shown that such molecular dynamics are the result of synergistic guest A−host water−guest B (CO_2−H_2O−THF) hydrogen-bonding interactions. Also, using molecular dynamics simulations performed at elevated temperatures (310, 315, and 320 K) and at a pressure of 100 MPa, Liang et al.[30] reported mechanisms of CO_2 migration within CO_2 CHs and suggested that for the diffusion of CO_2 molecules through five-membered water rings of the 5^{12} cage, at least one water vacancy is required, and for CO_2 molecules to pass through the six-membered water rings of the $5^{12}6^2$ cage, only a slight distortion of the local ring structure is sufficient. Such molecular migrations suggest that host−guest interaction in molecular solids can create a conducive environment for

Received: February 9, 2023
Accepted: March 10, 2023
Published: March 13, 2023

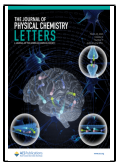

https://doi.org/10.1021/acs.jpclett.3c00373
J. Phys. Chem. Lett. 2023, 14, 2823−2829

chemical transformations. However, similar observations (for vapor-deposited ice film) under UHV and at extremely low temperatures as reported in this work have not been explored. Chemical evolution in interstellar ices depends mostly on the migration of reacting atoms and molecules at cryogenic temperatures. CH formation/dissociation in such conditions may provide mobility to the molecular species enabling chemical transformation. Also, the interstellar medium is expected to be more complex because a variety of clathrate-forming molecules exist along with water. Various single and mixed CHs may form along with pure solids of CO_2 and other molecular species, including CH_4, CO, CH_3OH, and NH_3 that exist there. Thus, preparing mixed CH and studying guest migration under UHV and cryogenic conditions may have implications for astrophysical and prebiotic science. While CO_2[6] and THF[13] CHs are reported to form in UHV, during thermal annealing, these CH cages are likely to undergo molecular exchange leading to the structural evolution of cages. In this study, we have used a custom-built UHV setup,[31] illustrated in Figure 1, to investigate the evolution of clathrate cages of CO_2 during the formation of THF CH under UHV and cryogenic temperatures.

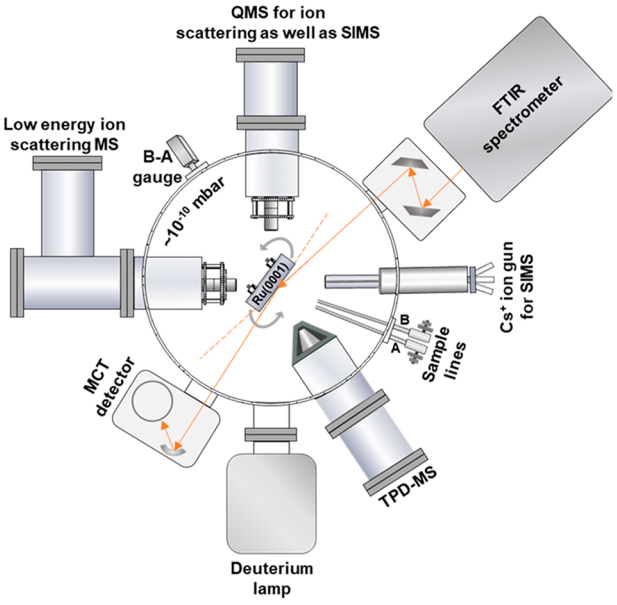

Figure 1. Schematic diagram of the experimental setup. In the schematic, the surface is oriented to do RAIR measurements.

To understand the evolution of clathrate cages of CO_2, we first prepared $CO_2@5^{12}$ and $CO_2@5^{12}6^2$. Figures 2A,B show the temperature-dependent RAIR spectra of 300 ML $CO_2@H_2O$ (150@150 ML) layered film in the C═O antisymmetric stretching region in the 90−150 K window. Spectra in a broader temperature window of 10−150 K are shown in Figure S1. Figures 2A,B show two IR peaks at 2348 and 2341 cm^{-1} at 90 K, which are assigned to the CO_2 encased in small 5^{12} ($CO_2@5^{12}$) and large $5^{12}6^2$ ($CO_2@5^{12}6^2$) cages of sI, respectively. The observed frequencies are comparable to the previous reports (2346, 2337 cm^{-1}),[1,2] where CH was grown by molecular deposition of water−guest gaseous mixtures in a vacuum at cryogenic temperatures. The frequency separation for the $CO_2@5^{12}$ and $CO_2@5^{12}6^2$ cages in this study is ∼7 cm^{-1}, which is comparable to ∼9 cm^{-1} of the previous report.[1] Notably, at 90 K, the peaks at 2348 and 2341 cm^{-1} have full width at half-maximum (FWHM) values of 3.4 and 6.7 cm^{-1}, respectively (shown in Figure S2), which are comparable to the FWHM values of 4 cm^{-1} (for $CO_2@5^{12}$ cages) and 8 cm^{-1} (for $CO_2@5^{12}6^2$ cages) of the previous report.[2] Furthermore, we have confirmed the formation of $CO_2@5^{12}$ and $CO_2@5^{12}6^2$ cages using quantum chemical simulations (see later). Based on the above observations, the 2348 and 2341 cm^{-1} peaks are assigned to $CO_2@5^{12}$ and $CO_2@5^{12}6^2$ cages, respectively. This partitioning of CO_2 in different CH cages at 90 K without the "help guest" molecules (THF, ethylene oxide, etc.) is seen for the first time in UHV.[1,2,9] However, upon annealing the sample above 90 K (also presented as contour plot in Figure 2B), the intensities of both the peaks (2348 and 2341 cm^{-1}) decreased proportionally before vanishing completely at 150 K due to the dissociation of the CH.

In one of our previous studies,[6] we had reported that in a codeposited mixture of CO_2 and H_2O ice at 10 K under UHV, CO_2 primarily occupies 5^{12} cages (2346 cm^{-1}) of sI along with a fraction of untrapped CO_2 (2353 cm^{-1}) that exists in the pores of the amorphous water matrix. However, in this study, a peak at ∼2382 cm^{-1} was observed for the sequentially deposited $CO_2@H_2O$ layered film at 10 K (Figure S1). This peak is assigned to the multilayer CO_2 ice film (compared to the spectrum of 150 ML of pure CO_2 film, Figure S3). The peak at 2382 cm^{-1} in the C═O antisymmetric stretching region did not change significantly during annealing the sample up to 80 K (Figure S1). However, at 90 K, the temperature at which pure CO_2 desorbs, most of the CO_2 diffuses through the water matrix and desorbs, leaving only a small fraction of it in the ice matrix that were later encaged in CH cages. The annealing temperature and associated mobility of CO_2 (mainly induced due to UHV environment) are crucial for forming the CH structure at 90 K. A shift in the C═O antisymmetric stretching region from ∼2382 cm^{-1} at a lower temperature to a doublet (2348 and 2341 cm^{-1}) at 90 K suggests CO_2 diffusion into the water matrix and interaction with water. This frequency shift was noted to be abrupt between 80 and 90 K (Figure S1).

We conducted a time-dependent RAIR experiment using a 300 ML $CO_2@H_2O$ layered film at 80 K to further understand this abrupt frequency change, or, in other words, diffusion of CO_2 into the water matrix and subsequent CH formation. The corresponding IR spectra at 80 K in the C═O antisymmetric stretching region are shown in Figures 2C,D. At 0 min, a peak at ∼2382 cm^{-1} was observed and was assigned to the multilayer film of CO_2.[6] Upon annealing the sample at the same temperature under UHV for several hours, the peak at 2382 cm^{-1} changes its shape and position with time due to the diffusion and desorption of CO_2 through the ice matrix. In other words, this band's evolution and shift are directly related to the thickness of the multilayer CO_2 film.[32] In addition, to confirm this, IR spectra of pure CO_2 ice of different thicknesses (2−150 ML) in the C═O antisymmetric stretching region at 10 K were collected as shown in Figure S4. The IR spectra in Figure S4 suggest that the intermediate spectra in Figures 2C,D are because of the different (reduced) thicknesses of the CO_2 film. This is because, at 80 K, in the $CO_2@H_2O$ (150@150 ML) layered film, CO_2 molecules diffuse into water matrix. The shift and shape change in the C═O antisymmetric stretching region were observed until ∼3 h (see the contour plot, Figure 2D). Finally, the 2382 cm^{-1} peak was shifted to 2348 and 2341 cm^{-1} and remained there until the end of the experiment (6 h). These observations suggest that CO_2 in the

https://doi.org/10.1021/acs.jpclett.3c00373
J. Phys. Chem. Lett. 2023, 14, 2823−2829

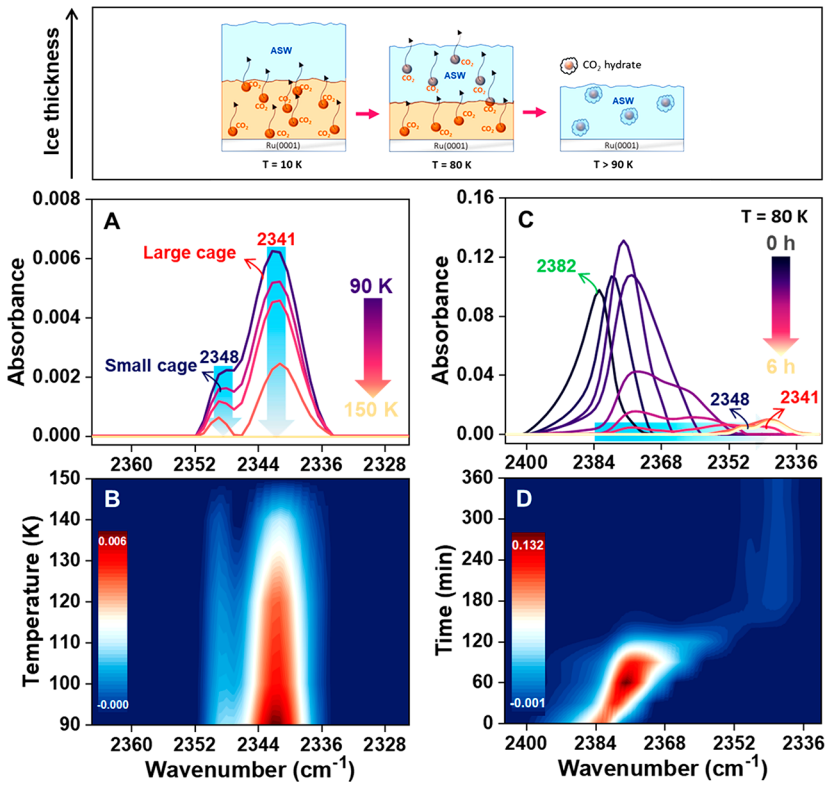

Figure 2. (A, B) Temperature-dependent RAIR spectra of 300 ML CO_2@H_2O (150@150 ML) layered film in the 90−150 K window in the C═O antisymmetric stretching region. (C, D) Time-dependent RAIR spectra of 300 ML CO_2@H_2O (150@150 ML) layered film at 80 K in the C═O antisymmetric stretching region. The peak at 2382 cm^{-1} (at 0 min) evolved with time and finally resulted in the twin peaks at 2348 and 2341 cm^{-1} after 3 h. The ice samples were created by vapor deposition at 10 K and further annealed to the set temperatures at an annealing rate of 2 K min^{-1}. Thermal annealing of the as-prepared sample and corresponding physical changes in ice matrix are schematically illustrated in the top panel.

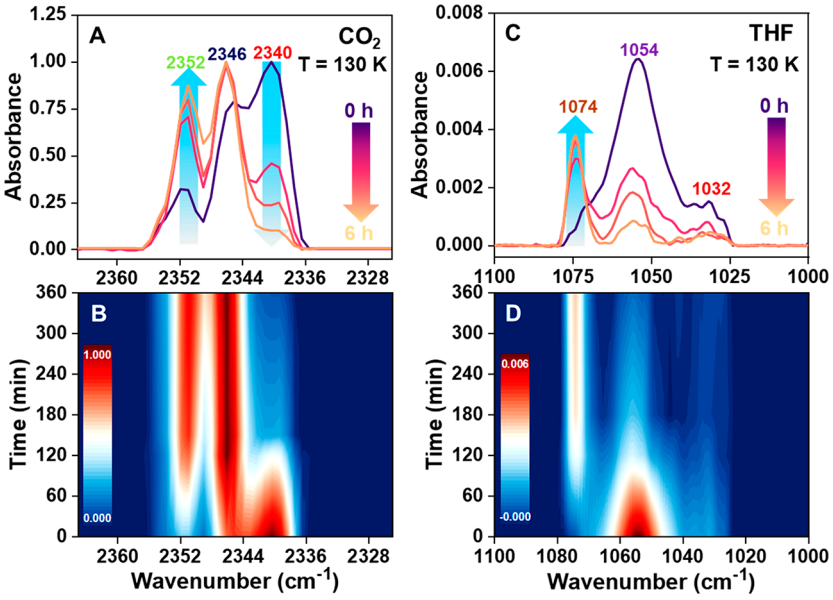

Figure 3. (A, B) Normalized time-dependent RAIR spectra of 300 ML CO_2@(THF+H_2O; 1:5) ice film at 130 K in the C═O antisymmetric stretching region of CO_2. (C, D) Time-dependent RAIR spectra of the same system in the C−O antisymmetric stretching region of THF. The ice sample was created by vapor deposition at 10 K and further annealed to 130 K at an annealing rate of 2 K min^{-1}.

layered CO_2@H_2O film near its desorption temperature diffuses through the water matrix (illustrated schematically in the top panel of Figure 2), and the enhanced mobility of CO_2 leads to its insertion into the different CH cages formed simultaneously at ∼90 K.

To examine the host−guest dynamics under UHV at cryogenic temperatures, we have chosen two guests, CO_2 and THF, and prepared 300 ML of CO_2@(THF+H_2O; 1:5) composite film at 10 K. See the Experimental Section for details of sample preparation. The resulting ice sample was

https://doi.org/10.1021/acs.jpclett.3c00373
J. Phys. Chem. Lett. 2023, 14, 2823−2829

annealed to 130 K and held there for 6 h to create mixed CO_2−THF CH. However, during annealing (of the sample from 10 to 130 K), initially CO_2 diffuses into the THF+H_2O (1:5) ice matrix, and at ∼90 K it forms classical sI hydrate forming the CO_2@5^{12} and CO_2@$5^{12}6^2$ cages (2348 and 2341 cm^{-1}, as shown in Figure 2). Figure 3 presents the time-dependent RAIR spectra of 300 ML of CO_2@(THF+H_2O; 1:5) composite film at 130 K in the C═O antisymmetric stretching region (A, B) of solid CO_2 and C−O antisymmetric stretching region (C, D) of solid THF. At 0 h, the spectra in Figures 3A,B show three peaks at 2352, 2346, and 2340 cm^{-1} in the C═O antisymmetric stretching region that are assigned to CO_2 in amorphous ice matrix, CO_2@5^{12}, and CO_2@$5^{12}6^2$ cages, respectively.[1,6] However, upon annealing the sample at 130 K for 6 h, the peak at 2340 cm^{-1} decreases and that at 2352 cm^{-1} increases, while that at 2346 cm^{-1} remains unaltered. This means that the CO_2 in the CO_2@$5^{12}6^2$ cages are being transported to the matrix of ASW and CO_2@5^{12} cages remain mostly unperturbed in the course of time. Simultaneously, in the C−O antisymmetric stretching region of THF in Figures 3C,D, a new peak arises at 1074 cm^{-1} while the peaks at 1054 and ∼1032 cm^{-1} decrease within a similar time scale. The peak at 1074 cm^{-1} is the characteristic peak for THF encased in $5^{12}6^4$ CH (THF@$5^{12}6^4$) cages, whereas the peaks at 1054 and ∼1032 cm^{-1} are assigned to THF trapped in amorphous water pores.[2,7,13,33] Therefore, at 130 K with time, the encased CO_2 is leaving the CO_2@$5^{12}6^2$ cages (reduction in the intensity of the 2340 cm^{-1} peak) while THF is forming the $5^{12}6^4$ cages (emergence of the 1074 cm^{-1} peak); also, the CO_2 molecules that vacated the $5^{12}6^2$ cages moved to the amorphous water matrix (this was confirmed by the emergence of the 2352 cm^{-1} peak). Hence, the formation of THF CH enhanced the mobility of CO_2 molecules into the water matrix. Also, the empty clathrate cages (CO_2@$5^{12}6^2$ cage in the current case) are inherently unstable, and partial dissociation of the same (which will further enhance the mobility of water molecules) might synergistically help the formation of pure THF CH (or a mixed CO_2−THF CH) at 130 K. This is because the thermodynamic stability of THF CH is superior compared to CO_2 CH.[34] Additionally, the formation of CO_2@5^{12} and THF@$5^{12}6^4$ cages was confirmed by calculating the vibrational frequencies of guests in the respective cages, and the obtained results are discussed below.

In addition, we have performed two control experiments to examine the role of THF CH and temperature on the migration of CO_2 in the water matrix under UHV. In the first experiment, we created 300 ML of CO_2@(THF+H_2O; 1:5) composite ice film at 10 K. The resulting sample was annealed to 120 K and held there for 6 h; the results are shown in Figure S5. During annealing at 120 K, neither the 1074 cm^{-1} peak (in the C−O antisymmetric stretching region of THF) nor the 2352 cm^{-1} peak (in the C═O antisymmetric stretching region of CO_2) appears, contrary to the results shown in Figures 3A,C. This suggests that at 120 K, neither THF CH forms nor CO_2 migrates into the water matrix. In the second experiment, we created pure CO_2 CH by annealing the CO_2@H_2O layered film (as discussed in Figure 2) at ∼90 K. Then the sample was further annealed to 130 K and held there for 6 h; the result is shown in Figure S6. We observed that the peaks at 2348 and 2341 cm^{-1} in the C═O antisymmetric stretching region decreased proportionally due to the dissociation of CH and desorption of CO_2 at 130 K. However, a decrease in the peak at 2341 cm^{-1} (due to CO_2@$5^{12}6^2$) alone and the appearance of peak at 2352 cm^{-1} (CO_2 in ASW) were not observed. This suggests that in the absence of THF CH, CO_2 does not migrate into the water matrix. Therefore, these two control experiments suggest that the THF CH formation in a water matrix containing CO_2 CH is crucial for the mobility of CO_2 under UHV and at 130 K.

In addition, the mobility of H_2O molecules during CH formation/dissociation was monitored for CO_2@H_2O and CO_2@(THF+H_2O; 1:5) films in the O−H stretching region at 130 K; the results are shown in Figure S7. We observed that after 6 h the change in the shape of the O−H stretching region was not significant for pure CO_2 CH (Figure S7A) as it was observed for mixed CH of CO_2 with THF (Figure S7B). The change in shape of the O−H stretching band depicts the ordering/reorientation of water molecules in the ice matrix;[35] a similar result has been observed in our previous reports.[13,36,37] The higher mobility of water in the case of the CO_2@(THF+H_2O; 1:5) composite ice film is reasonable because at 130 K the following events occur: (1) formation of THF CH, (2) dissociation of CO_2 CH (CO_2@$5^{12}6^2$ cages), and (3) migration of CO_2 molecules into the water matrix.

Fleyfel and Devlin[2] have reported the epitaxial growth of sI CO_2 hydrate on ethylene oxide hydrate and sII CO_2 hydrate on THF hydrate under vacuum. For epitaxial growth, the resulting CH structure of CO_2 depends on the type of "help guest" and its base structure. However, in the current study, the results presented in Figure 2 clearly demonstrate the partitioning of CO_2 in CO_2@5^{12} and CO_2@$5^{12}6^2$ cages of sI at 90 K without the help guest. In UHV, such a result has not been reported earlier. In addition, when we introduced THF in the CO_2@H_2O film, CO_2@(THF+H_2O; 1:5), and annealed the resulting ice, we observed a unusual situation where at 130 K the water matrix contains THF as well as CO_2@5^{12} and CO_2@$5^{12}6^2$ cages. Moudrakovski et al.[27] have presented evidence for cage-to-cage transport of CO_2, when THF and CO_2 were guests in the $5^{12}6^4$ and 5^{12} cages of sII hydrate, respectively. They have suggested that this is because of the synergistic hydrogen-bonding interactions of THF and CO_2 with the water lattice that promoted the injection of Bjerrum defects, which in turn enabled faster water reorientation. In present study at 130 K, after initial THF CH (THF@$5^{12}6^4$ cage) formation, caged THF can undergo hydrogen-bonding interaction with CO_2 of both the CO_2@5^{12} and CO_2@$5^{12}6^2$ cages. However, the results presented in Figure 3A demonstrate the migration of CO_2 from CO_2@$5^{12}6^2$ cages alone. Here, we have two possibilities: (1) As suggested by Liang et al.[30] that for CO_2 molecules to move from the $5^{12}6^2$ cage, only a slight distortion of the local ring structure is sufficient, compared to the case of the 5^{12} cage, where one water vacancy is required. This suggests that the interaction of THF with water of the $5^{12}6^2$ cage may provide the required distortion to the local ring structure for CO_2 migration from the CO_2@$5^{12}6^2$ cages. A similar experimental result has been reported by Devlin and Monreal.[38] In mixed CO_2−THF sII CH, they observed[38] that over a 5 h period, CO_2 moves from the CO_2@$5^{12}6^2$ cage and additional CO_2@5^{12} cage arises at 116 K. (2) It is possible that caged THF may interact with the CO_2 of both the 5^{12} and $5^{12}6^2$ cages, enabling the migration to CO_2 of both the cages to the water matrix as suggested by Moudrakovski et al.[27] This suggests that primarily CO_2 molecules from both the cages are migrating; in other words, CH cages are dissociating. However, in the presence of THF@$5^{12}6^4$ cages, the 5^{12} cages are being occupied by CO_2. Further

https://doi.org/10.1021/acs.jpclett.3c00373
J. Phys. Chem. Lett. 2023, 14, 2823−2829

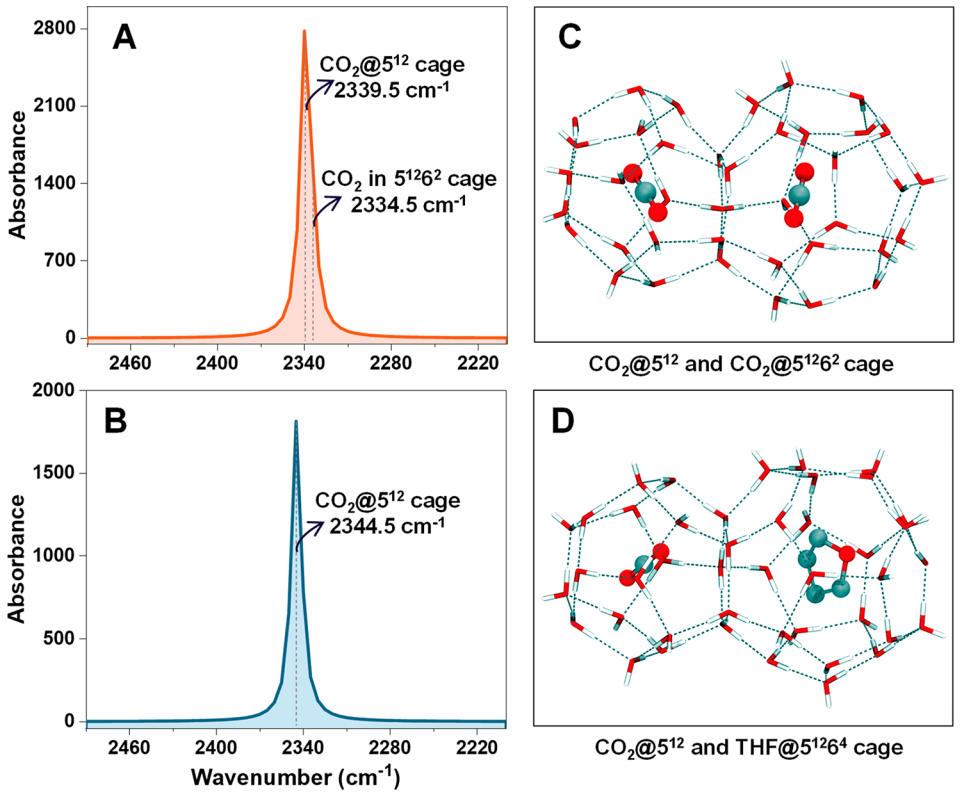

Figure 4. Computed IR spectra in the C═O antisymmetric stretching region of CO_2. (A) When CO_2 was sequentially added in one small 5^{12} and one large $5^{12}6^2$ cage of sI. (B) When CO_2 and THF were sequentially added in one small 5^{12} and one large $5^{12}6^4$ cage of the sII, the result is shown only for encased CO_2 in the 5^{12} cage. IR spectra were generated from fully optimized CH structures along with the guest molecules; the optimized structures of CH cages are shown in (C) and (D).

experimental and computational studies are required to decipher the exact mechanism of CO_2 migration in the presence of THF under UHV conditions.

If we compare the IR peaks for the CO_2@5^{12} cage in water matrix with and without THF, they are at 2346 and 2348 cm^{-1}, respectively. This suggests that there is a structural change[2,22] in the presence of THF. At lower temperature, when THF is not mobile, the diffusing CO_2 forms sI hydrate, and with increase in temperature when THF is mobile, formation of sII hydrate was observed. It should be noted that the IR spectral resolution employed in the work was 2 cm^{-1}. The change in vibrational frequency of the CO_2@5^{12} cage in presence and absence of THF is computed, and the results are discussed below.

We confirmed the formation of pure CO_2 CH (CO_2@5^{12} and CO_2@$5^{12}6^2$) and mixed CH of CO_2 with THF (CO_2@5^{12} and THF@$5^{12}6^4$) using quantum chemical calculations. The optimized geometries and corresponding vibrational frequencies for different CH structures in the C═O antisymmetric stretching region of CO_2 are shown in Figure 4. For pure CO_2 CH, the relevant computed vibrational frequencies for CO_2@5^{12} and CO_2@$5^{12}6^2$ cages are 2339.5 and 2334.5 cm^{-1}, respectively, as shown in Figure 4A. The frequency shift between two peaks (of CO_2@5^{12} and CO_2@$5^{12}6^2$ cages) obtained in computational and experimental studies are ∼5 and ∼7 cm^{-1}, respectively (Table S1). Thus, the computationally determined vibrational frequencies in the C═O antisymmetric stretching region during hydrate formation closely match with the experimental values shown in Figure 2A. Similarly, for mixed CH of CO_2 with THF, the computed vibrational frequencies for CO_2@5^{12} and THF@$5^{12}6^4$ cages are 2344.5 cm^{-1} (in the C═O antisymmetric stretching region of CO_2) and 1087 cm^{-1} (in the C−O antisymmetric stretching region of THF). These computed results agree well with the experimental results shown in Figures 3A,C and are listed in Table S2. The computed IR spectrum for the CO_2@5^{12} cage of mixed CH of CO_2−THF is shown in Figure 4B. If we compare the computed vibrational frequencies for the CO_2@5^{12} cage with and without THF in an adjacent cage, they are at 2344.5 and 2339.5 cm^{-1}, respectively. This suggest that THF is indeed playing a crucial role in structural evolution of CO_2 CH. Here, all the calculations were done by considering the small and large cages of CH structures adjoining each other. The coordinates of the optimized geometries of pure CO_2 CH (CO_2@5^{12} and CO_2@$5^{12}6^2$ cages) and mixed CH of CO_2−THF (CO_2@5^{12} and THF@$5^{12}6^4$ cages) are given in Tables S3 and S4.

The CO_2 dynamics in the presence of polar THF discussed in this work can be extended for several other guest molecules to understand the molecular mobility and structural evolution of CH cages in such molecular solids under UHV and cryogenic conditions. Such molecular mobility could lead to new reaction pathways for chemical transformation. For example, when CO_2 (or other guest molecule) is encased, these CO_2 molecules are perhaps not available for any reaction. However, if these molecules come out of cages under certain circumstances as the present work suggests, new chemical pathways are possible, which would lead to new possibilities of chemical evolution.

In this study, we observed the migration of CO_2 from $5^{12}6^2$ CH cages to the bulk of ASW in the presence of THF at 130 K in UHV. Continuous evolution of CH structures and the

https://doi.org/10.1021/acs.jpclett.3c00373
J. Phys. Chem. Lett. 2023, 14, 2823−2829

corresponding changes in the ice matrix imply rapid structural dynamics and flexibility of the ice matrix, possibly similar to liquid-like order at 130 K, in UHV. This CH cage-to-matrix exchange of molecules suggests an active environment in these molecular solids that enables mobility of the species for chemical transformations, specially with additional activation. The structural evolution in mixed CHs implies mechanical changes in the system, although the time scale of this process has not been examined. It occurs faster than the time needed for spectral measurements (<2 s) so that all the species are captured in one spectrum.

■ ASSOCIATED CONTENT

Supporting Information

The Supporting Information is available free of charge at https://pubs.acs.org/doi/10.1021/acs.jpclett.3c00373.

Experimental Section (including experimental setup, materials and reagents, sample preparation, experimental procedure, RAIRS setup, and computational details); temperature-dependent/time-dependent RAIR spectra of pure CO_2, CO_2@H_2O, and CO_2@(THF+H_2O; 1:5) films; comparison of the experimental and computational vibrational frequencies (Tables S1 and S2) and Cartesian coordinates (Tables S3 and S4) for pure CO_2 CH and mixed CH of CO_2 and THF (PDF)

■ AUTHOR INFORMATION

Corresponding Authors

Thalappil Pradeep − *DST Unit of Nanoscience (DST UNS) and Thematic Unit of Excellence (TUE), Department of Chemistry, Indian Institute of Technology Madras, Chennai 600036, India; International Centre for Clean Water, IIT Madras Research Park, Chennai 600113, India;* orcid.org/0000-0003-3174-534X; Email: pradeep@iitm.ac.in

Rajnish Kumar − *Department of Chemical Engineering, Indian Institute of Technology Madras, Chennai 600036, India; International Centre for Clean Water, IIT Madras Research Park, Chennai 600113, India;* orcid.org/0000-0002-4172-2638; Email: rajnish@iitm.ac.in

Sandeep K. Reddy − *Centre for Computational and Data Science, Indian Institute of Technology Kharagpur, Kharagpur, West Bengal 721302, India;* orcid.org/0000-0002-1458-6853; Email: skreddy@iitkgp.ac.in

Authors

Gaurav Vishwakarma − *DST Unit of Nanoscience (DST UNS) and Thematic Unit of Excellence (TUE), Department of Chemistry, Indian Institute of Technology Madras, Chennai 600036, India*

Bijesh K. Malla − *DST Unit of Nanoscience (DST UNS) and Thematic Unit of Excellence (TUE), Department of Chemistry, Indian Institute of Technology Madras, Chennai 600036, India*

K. S. S. V. Prasad Reddy − *Department of Chemistry, Indian Institute of Technology Madras, Chennai 600036, India*

Jyotirmoy Ghosh − *Department of Chemistry, Purdue University, West Lafayette, Indiana 47907, United States*

Soham Chowdhury − *DST Unit of Nanoscience (DST UNS) and Thematic Unit of Excellence (TUE), Department of Chemistry, Indian Institute of Technology Madras, Chennai 600036, India*

Sharma S. R. K. C. Yamijala − *Department of Chemistry and Centre for Atomistic Modelling and Materials Design, Centre for Quantum Information, Communication, and Computing, and Centre for Molecular Materials and Functions, Indian Institute of Technology Madras, Chennai 600036, India;* orcid.org/0000-0003-1773-9226

Complete contact information is available at: https://pubs.acs.org/10.1021/acs.jpclett.3c00373

Author Contributions

G.V. and T.P. designed the research; G.V., B.K.M., and S.C. performed the experiments; K.S.S.V.P.R, S.S.R.K.Y., and S.K.R. performed the quantum chemical calculations; G.V., B.K.M., K.S.S.V., J.G., S.C., S.S.R.K.Y., S.K.R., R.K., and T.P. analyzed data; and G.V., B.K.M., R.K., and T.P. wrote the paper.

Notes

The authors declare no competing financial interest.

■ ACKNOWLEDGMENTS

We acknowledge the Science and Engineering Research Board (SERB), Department of Science and Technology (DST), Government of India, for research funding. T.P. and R. K. acknowledge funding from the Centre of Excellence on Molecular Materials and Functions under the Institution of Eminence scheme of IIT Madras. S.K.R. acknowledges the ISIRD award, IIT Kharagpur for the financial support and the National Supercomputing Mission (NSM) for providing computing resources of "PARAM Shakti" at IIT Kharagpur, which is implemented by C-DAC and supported by the Ministry of Electronics and Information Technology (MeitY) and Department of Science and Technology (DST), Government of India. S.S.R.K.C.Y. acknowledges the financial support of IIT Madras through its new faculty support grants NFSG (IP2021/0972CY/NFSC008973), NFIG (RF2021/0577CY/NFIG 008973), and DST-SERB (SRG/2021/001455). G.V. and S.C. thank IITM for their research fellowship. B.K.M. thanks the University Grants Commission (UGC) for his research fellowship.

■ REFERENCES

(1) Fleyfel, F.; Devlin, J. P. FT-IR Spectra of 90 K Films of Simple, Mixed, and Double Clathrate Hydrates of Trimethylene Oxide, Methyl Chloride, Carbon Dioxide, Tetrahydrofuran, and Ethylene Oxide Containing Decoupled D2O. *J. Phys. Chem.* **1988**, *92* (3), 631−635.

(2) Fleyfel, F.; Devlin, J. P. Carbon Dioxide Clathrate Hydrate Epitaxial Growth: Spectroscopic Evidence for Formation of the Simple Type-II Carbon Dioxide Hydrate. *J. Phys. Chem.* **1991**, *95* (9), 3811−3815.

(3) Hallbrucker, A. A Clathrate Hydrate of Nitric Oxide. *Angew. Chemie Int. Ed.* **1994**, *33* (6), 691−693.

(4) Hallbrucker, A.; Mayer, E. Unexpectedly Stable Nitrogen, Oxygen, Carbon Monoxide and Argon Clathrate Hydrates from Vapour-Deposited Amorphous Solid Water: An X-Ray and Two-Step Differential Scanning Calorimetry Study. *J. Chem. Soc. Faraday Trans.* **1990**, *86* (22), 3785−3792.

(5) Mayer, E.; Hallbrucker, A. Unexpectedly Stable Nitrogen and Oxygen Clathrate Hydrates from Vapour Deposited Amorphous Solid Water. *Chem. Commun.* **1989**, No. 12, 749−751.

(6) Ghosh, J.; Methikkalam, R. R. J.; Bhuin, R. G.; Ragupathy, G.; Choudhary, N.; Kumar, R.; Pradeep, T. Clathrate Hydrates in Interstellar Environment. *Proc. Natl. Acad. Sci. U. S. A.* **2019**, *116* (5), 1526−1531.

(7) Monreal, I. A.; Devlin, J. P.; Maşlakcı, Z.; Cicek, M. B.; Uras-Aytemiz, N. Controlling Nonclassical Content of Clathrate Hydrates through the Choice of Molecular Guests and Temperature. *J. Phys. Chem. A* **2011**, *115* (23), 5822−5832.
(8) Bauer, R. P. C.; Ravichandran, A.; Tse, J. S.; Appathurai, N.; King, G.; Moreno, B.; Desgreniers, S.; Sammynaiken, R. In Situ X-Ray Diffraction Study on Hydrate Formation at Low Temperature in a High Vacuum. *J. Phys. Chem. C* **2021**, *125* (48), 26892−26900.
(9) Netsu, R.; Ikeda-Fukazawa, T. Formation of Carbon Dioxide Clathrate Hydrate from Amorphous Ice with Warming. *Chem. Phys. Lett.* **2019**, *716*, 22−27.
(10) Ripmeester, J. A.; Ding, L.; Klug, D. D. A Clathrate Hydrate of Formaldehyde. *J. Phys. Chem.* **1996**, *100* (32), 13330−13332.
(11) Richardson, H. H.; Wooldridge, P. J.; Devlin, J. P. FT-IR Spectra of Vacuum Deposited Clathrate Hydrates of Oxirane H 2S, THF, and Ethane. *J. Chem. Phys.* **1985**, *83* (9), 4387−4394.
(12) Blake, D.; Allamandola, L.; Sandford, S.; Hudgins, D.; Freund, F. Clathrate Hydrate Formation in Amorphous Cometary Ice Analogs in Vacuo. *Science* **1991**, *254* (5031), 548−551.
(13) Ghosh, J.; Bhuin, R. G.; Ragupathy, G.; Pradeep, T. Spontaneous Formation of Tetrahydrofuran Hydrate in Ultrahigh Vacuum. *J. Phys. Chem. C* **2019**, *123*, 16300−16307.
(14) Malla, B. K.; Vishwakarma, G.; Chowdhury, S.; Selvarajan, P.; Pradeep, T. Formation of Ethane Clathrate Hydrate in Ultrahigh Vacuum by Thermal Annealing. *J. Phys. Chem. C* **2022**, *126*, 17983.
(15) Ghosh, J.; Bhuin, R. G.; Vishwakarma, G.; Pradeep, T. Formation of Cubic Ice via Clathrate Hydrate, Prepared in Ultrahigh Vacuum under Cryogenic Conditions. *J. Phys. Chem. Lett.* **2020**, *11* (1), 26−32.
(16) Ghosh, J.; Vishwakarma, G.; Das, S.; Pradeep, T. Facile Crystallization of Ice I_h via Formaldehyde Hydrate in Ultrahigh Vacuum under Cryogenic Conditions. *J. Phys. Chem. C* **2021**, *125* (8), 4532−4539.
(17) Dartois, E. CO Clathrate Hydrate: Near to Mid-IR Spectroscopic Signatures. *Icarus* **2011**, *212* (2), 950−956.
(18) Ghosh, J.; Methikkalam, R. R. J.; Bhuin, R. G.; Ragupathy, G.; Choudhary, N.; Kumar, R.; Pradeep, T. Reply to Choukroun et Al.: IR and TPD Data Suggest the Formation of Clathrate Hydrates in Laboratory Experiments Simulating ISM. *Proc. Natl. Acad. Sci. U. S. A.* **2019**, *116*, 14409−14410.
(19) Sloan, E. D. Fundamental Principles and Applications of Natural Gas Hydrates. *Nature* **2003**, *426*, 353−359.
(20) Walsh, M. R.; Koh, C. A.; Sloan, D. E.; Sum, A. K.; Wu, D. T. Microsecond Simulations of Spontaneous Methane Hydrate Nucleation and Growth. *Science (80-.).* **2009**, *326* (5956), 1095−1098.
(21) Park, Y.; Kim, D. Y.; Lee, J. W.; Huh, D. G.; Park, K. P.; Lee, J.; Lee, H. Sequestering Carbon Dioxide into Complex Structures of Naturally Occurring Gas Hydrates. *Proc. Natl. Acad. Sci. U. S. A.* **2006**, *103* (34), 12690−12694.
(22) Kumar, R.; Lang, S.; Englezos, P.; Ripmeester, J. Application of the ATR-IR Spectroscopic Technique to the Characterization of Hydrates Formed by CO_2, CO_2/H2 and CO_2/H2/C3H8. *J. Phys. Chem. A* **2009**, *113* (22), 6308−6313.
(23) Davidson, D. W.; Ripmeester, J. A. NMR, NQR, and Dielectric Properties of Clathrates. In *Inclusion Compounds*; Atwood, J. L., Davies, J. E. D., MacNicol, D. D., Eds.; Academic Press: 1984; Vol. 3, pp 69−123.
(24) Ripmeester, J. A.; Ratcliffe, C. I. Solid State NMR Studies of Inclusion Compounds. In *Inclusion Compounds*; Atwood, J. L., Davies, J. E. D., MacNicol, D. D., Eds.; Oxford University Press: Oxford, 1991; Vol. 5, pp 37−85.
(25) Kirschgen, T. M.; Zeidler, M. D.; Geil, B.; Fujara, F. A Deuteron NMR Study of the Tetrahydrofuran Clathrate Hydrate Part II:† Coupling of Rotational and Translational Dynamics of Water. *Phys. Chem. Chem. Phys.* **2003**, *5* (23), 5247−5252.
(26) Davies, S. R.; Sloan, E. D.; Sum, A. K.; Koh, C. A. In Situ Studies of the Mass Transfer Mechanism across a Methane Hydrate Film Using High-Resolution Confocal Raman Spectroscopy. *J. Phys. Chem. C* **2010**, *114* (2), 1173−1180.
(27) Moudrakovski, I. L.; Udachin, K. A.; Alavi, S.; Ratcliffe, C. I.; Ripmeester, J. A. Facilitating Guest Transport in Clathrate Hydrates by Tuning Guest-Host Interactions. *J. Chem. Phys.* **2015**, *142* (7), 074705.
(28) Alavi, S.; Ripmeester, J. A. Hydrogen-Gas Migration through Clathrate Hydrate Cages. *Angew. Chemie - Int. Ed.* **2007**, *46* (32), 6102−6105.
(29) Takeya, S.; Ripmeester, J. A. Dissociation Behavior of Clathrate Hydrates to Ice and Dependence on Guest Molecules. *Angew. Chemie - Int. Ed.* **2008**, *47* (7), 1276−1279.
(30) Liang, S.; Liang, D.; Wu, N.; Yi, L.; Hu, G. Molecular Mechanisms of Gas Diffusion in CO_2 Hydrates. *J. Phys. Chem. C* **2016**, *120* (30), 16298−16304.
(31) Bag, S.; Bhuin, R. G.; Methikkalam, R. R. J.; Pradeep, T.; Kephart, L.; Walker, J.; Kuchta, K.; Martin, D.; Wei, J. Development of Ultralow Energy (1−10 EV) Ion Scattering Spectrometry Coupled with Reflection Absorption Infrared Spectroscopy and Temperature Programmed Desorption for the Investigation of Molecular Solids. *Rev. Sci. Instrum.* **2014**, *85* (1), No. 014103.
(32) Escribano, R. M.; Caro, G. M. M.; Cruz-Diaz, G. A.; Rodríguez-Lazcano, Y.; Maté, B. Crystallization of CO_2 Ice and the Absence of Amorphous CO_2 Ice in Space. *Proc. Natl. Acad. Sci. U. S. A.* **2013**, *110* (32), 12899−12904.
(33) Monreal, I. A.; Cwiklik, L.; Jagoda-Cwiklik, B.; Devlin, J. P. Classical to Nonclassical Transition of Ether-HCN Clathrate Hydrates at Low Temperature. *J. Phys. Chem. Lett.* **2010**, *1* (1), 290−294.
(34) Babu, P.; Linga, P.; Kumar, R.; Englezos, P. A Review of the Hydrate Based Gas Separation (HBGS) Process Forcarbon Dioxide Pre-Combustion Capture. *Energy* **2015**, *85*, 261−279.
(35) Backus, E. H. G.; Grecea, M. L.; Kleyn, A. W.; Bonn, M. Surface Crystallization of Amorphous Solid Water. *Phys. Rev. Lett.* **2004**, *92* (23), 236101.
(36) Vishwakarma, G.; Ghosh, J.; Pradeep, T. Desorption-Induced Evolution of Cubic and Hexagonal Ices in an Ultrahigh Vacuum and Cryogenic Temperatures. *Phys. Chem. Chem. Phys.* **2021**, *23* (41), 24052−24060.
(37) Vishwakarma, G.; Malla, B. K.; Methikkalam, R. R. J.; Pradeep, T. Rapid Crystallization of Amorphous Solid Water by Porosity Induction. *Phys. Chem. Chem. Phys.* **2022**, *24* (42), 26200−26210.
(38) Devlin, J. P.; Monreal, I. A. Instant Conversion of Air to a Clathrate Hydrate: CO2 Hydrates Directly from Moist Air and Moist CO 2 (G). *J. Phys. Chem. A* **2010**, *114*, 13129−13133.

https://doi.org/10.1021/acs.jpclett.3c00373
J. Phys. Chem. Lett. 2023, 14, 2823−2829